Differential x-ray phase contrast imaging using a shearing interferometer

C. David, B. Nöhammer, H. H. Solak, and E. Ziegler

Citation: Applied Physics Letters **81**, 3287 (2002); doi: 10.1063/1.1516611
View online: http://dx.doi.org/10.1063/1.1516611
View Table of Contents: http://scitation.aip.org/content/aip/journal/apl/81/17?ver=pdfcov
Published by the AIP Publishing

Differential x-ray phase contrast imaging using a shearing interferometer

C. David,[a] B. Nöhammer, and H. H. Solak
Laboratory for Micro- and Nanotechnology, Paul Scherrer Institut, CH-5232 Villigen-PSI, Switzerland

E. Ziegler
European Synchrotron Radiation Facility, Boîte Postal 220, F-38043 Grenoble Cedex, France

(Received 2 May 2002; accepted 3 September 2002)

An x-ray interferometer has been developed that uses two transmission phase gratings to analyze wave front distortions in the hard x-ray range. The interferometer is insensitive to mechanical drift and vibrations, and it is tunable over a wide range of photon energies. This setup was used for differential phase contrast imaging of low-absorbing test objects. We obtained micrographs with moiré fringes of good visibility, which revealed the local phase shift gradient caused by the objects. A comparison with numerically simulated images indicates that quantitative analysis of unknown phase objects is possible. © *2002 American Institute of Physics.*
[DOI: 10.1063/1.1516611]

The phase-shift cross sections of light elements are much larger than the absorption cross sections in the x-ray region. Therefore, the acquisition of x-ray micrographs with sufficient contrast in amplitude requires a significantly higher radiation dose than phase contrast micrographs. A variety of x-ray techniques are employed to detect the phase contrast of a sample, i.e., to convert it into amplitude with contrast in the image plane. In soft x-ray microscopes a phase shifting plate in the back focal plane of a zone plate lens can be used for this.[1] For small phase shifts, this Zernicke-type phase contrast mechanism gives an intensity modulation that is in first approximation proportional to the phase shift of the object. Other techniques use the Fresnel diffraction of coherent hard x rays at the edges of a phase object to significantly improve the visibility of an object in microradiography.[2] In first approximation, the intensity distribution obtained is proportional to the Laplacian of the refractive index distribution,[3] and in certain cases reconstruction of a phase object from a single micrograph is possible.[4] Quantitative information on arbitrary phase objects can be obtained by numerically evaluating series of images acquired with the detector placed at different distances from the sample.[5]

The most sensitive method to measure the phase shifts introduced to a wave front is interferometry. A setup for a Mach–Zehnder-type interferometer operated in the hard x-ray range was introduced by Bonse and Hart[6] more than three decades ago. It consists of three partially transmitting Bragg crystals used as beam splitter and recombining elements. The incoming light is split into two separated branches one of which passes through the sample while the other serves as an unperturbed reference beam [see Fig. 1(a)]. The two beams interfering at the exit of the interferometer give an intensity distribution that represents the difference in optical path and thus, if perfectly aligned, of the phase shift caused by the object. Ando and Hosoya pioneered phase contrast imaging with such a device in the early 1970s,[7] and more recent setups have produced excellent phase contrast images and computer tomograms.[8,9] The main technical difficulty lies in the extreme demands for mechanical stability of the optical components, since the relative positions of the optical components have to be stable within a fraction of a lattice constant, i.e., to subangström dimensions. Therefore, Bonse–Hart interferometers are very difficult to handle especially when made big enough to investigate large samples.

We developed a different kind of interferometer, in which the interfering beams are not completely separated but merely are sheared by a small angle so that they pass through different, closely spaced parts of the sample. Figure 1(b) shows such a shearing interferometer consisting of three transmission gratings, analogous to the Bonse–Hart setup. The first grating splits the incoming wave into the $+1$st and -1st diffraction orders, which are then recombined by a second grating with half the pitch of the first grating. Downstream of the recombiner grating, the interference of the two wave fronts results in a pattern of interference lines. If an amplitude grating consisting of alternating opaque and transmitting lines with appropriate pitch and orientation is placed in the interference region, the position of the interference maxima with respect to the grating structures determines whether the radiation is mostly absorbed or transmitted. With a slight angular misalignment or mismatch of the grating

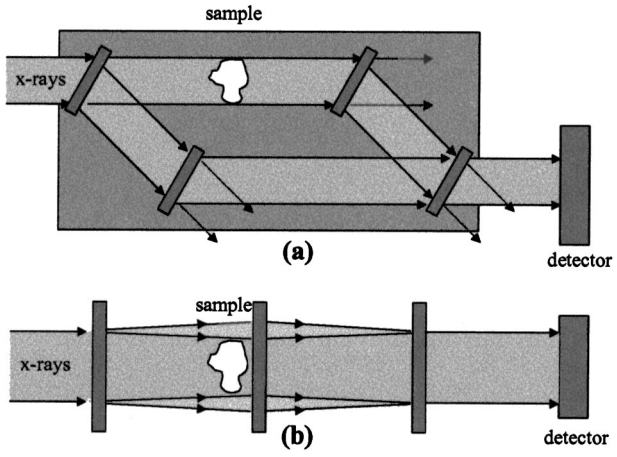

FIG. 1. Schematic of a Bonse–Hart interferometer (a) and a shearing interferometer (b).

[a]Electronic mail: christian.david@psi.ch

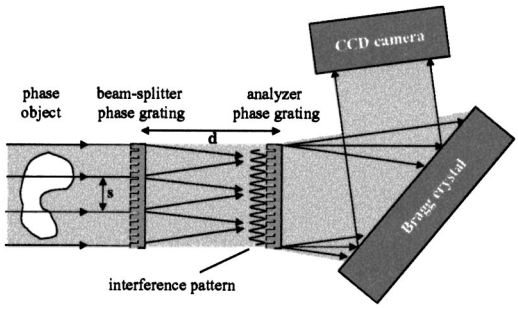

FIG. 2. Schematic of the shearing interferometer setup used that consisted of two phase gratings and a Bragg crystal.

pitch, a pattern of moiré lines will appear. A phase object placed between the first and third gratings can cause a difference in phase shift between two interfering beams, which in turn can be observed as a shift in the position of the interference line pattern. The intensity transmitted through the analyzer will therefore depend on the difference in phase shift introduced by two closely spaced regions of the sample, i.e., the gradient in phase shift. Thus, the resulting interferograms are differential phase contrast micrographs.

The experimental work presented in this letter was carried out using a modified setup (Fig. 2). First, we omitted the first (beam splitter) grating. This is possible when the spatial separation s between the two interfering beams in the plane of the phase object is smaller than the transverse coherence of the radiation. Second, we used two phase gratings as diffractive elements, since amplitude gratings with sufficiently fine pitch and high attenuation are very difficult to obtain because they require absorbing structures with extremely high aspect ratios. When a phase grating is used as an analyzer, the relative phase of the interfering waves determines how the incoming intensity will be distributed over the analyzer's diffraction orders. A Bragg crystal between the analyzer grating and the detector was used to select the 0th diffraction order to acquire the interferograms.

The phase gratings were fabricated by a method that we reported recently.[10] We used electron-beam lithography and anisotropic wet etching of ⟨110⟩ oriented silicon to obtain linear gratings with high aspect ratios. To minimize absorption losses, the Si structures were made on approximately 10 μm thick silicon membranes. Figure 3(a) shows one of the diffractive elements used in this experiment. The structures were made with a duty cycle close to 0.5, i.e., with equal

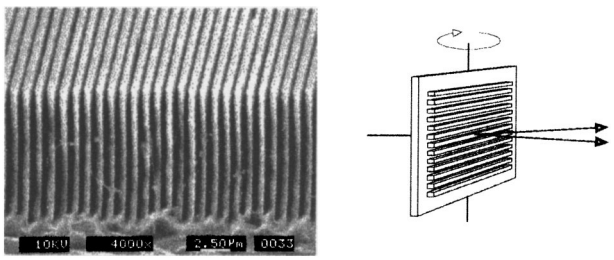

FIG. 3. Scanning electron microscopy micrograph of a silicon phase grating used in the shearing interferometer setup (a). The structures are 9.6 μm high. By tilting the structures with respect to the beam, the structure height can be tuned to obtain optimum efficiency (b).

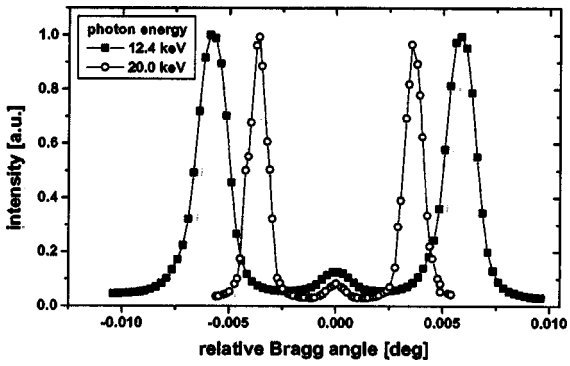

FIG. 4. Angular distribution of the intensity transmitted through a phase grating with 1 μm pitch obtained by scanning the Bragg angle of a Si ⟨111⟩ analyzer crystal. The grating was tilted 52.0° (for 12.4 keV) and 67.8° (for 20 keV). The curves are centered around their zero order peak.

lines and spaces to minimize the zero order transmission. As indicated in Fig. 3(b), the structure height and thus the phase shift introduced could be tuned to the optimum value of π over a wide range of photon energies by tilting the gratings relative to the incoming x-ray beam.[11]

We tested the interferometer on the optics beamline of the European Synchrotron Radiation Facility (ESRF) at 12.4 and 20.0 keV photon energy. The bending magnet radiation was monochromatized by a double crystal Si ⟨111⟩ monochromator. The optimum structure heights of a Si phase grating are 15.7 and 25.6 μm for 12.4 and 20.0 keV photon energies, respectively.

The performance of the beam splitter and analyzer gratings was investigated by measuring the flux transmitted into the 0th and $\pm$1st diffraction orders. Figure 4 shows the angular distribution of the intensity transmitted through the grating shown in Fig. 3. For both 12.4 and 20.0 keV photon energies, the 0th diffraction order has an approximately 10 times lower intensity compared to the $\pm$1st diffraction orders. This means that the $\pm$1st order diffraction efficiency is close to the theoretical optimum of a pure phase grating of 40.5%. The remaining 0th order intensity can be explained by minor mismatch of the gratings' duty cycle and by the fact that the Si structures are not solely phase shifting but also absorb a few percent of the incident radiation.

The transverse coherence length t of the incoming radiation is approximately given by $t \approx r\ \lambda/S$, where r represents the distance from the source, λ the x-ray wavelength, and S the source size. The separation s of the interfering beams is given by $s = 2\lambda d/p$, so the maximum separation $d_{\max}$ of the gratings which still maintains transverse coherence is given by $d_{\max} \approx rp/2S$, independent of the wavelength. In our case, the horizontal and vertical source sizes were $S_{\text{hor}} \approx 300$ μm and $S_{\text{ver}} \approx 80$ μm (FWHM). Therefore we chose to orient the gratings such that the interfering beams were separated in the vertical direction. For a source distance of $r = 40$ m and a grating pitch of $p = 1$ μm, the vertical transverse coherence limits the grating separation to a maximum of $d_{\max} \approx 200$ mm. The experiments presented were carried out at $d = 70$ mm, assuring ample transverse coherence.

As predicted, we detected patterns of moiré lines at both photon energies. The ratio of the maximum and minimum intensities of the fringe patterns was measured to be $I_{\max}/I_{\min} = 1.9$, resulting in a visibility of $(I_{\max} - I_{\min})/(I_{\max}$

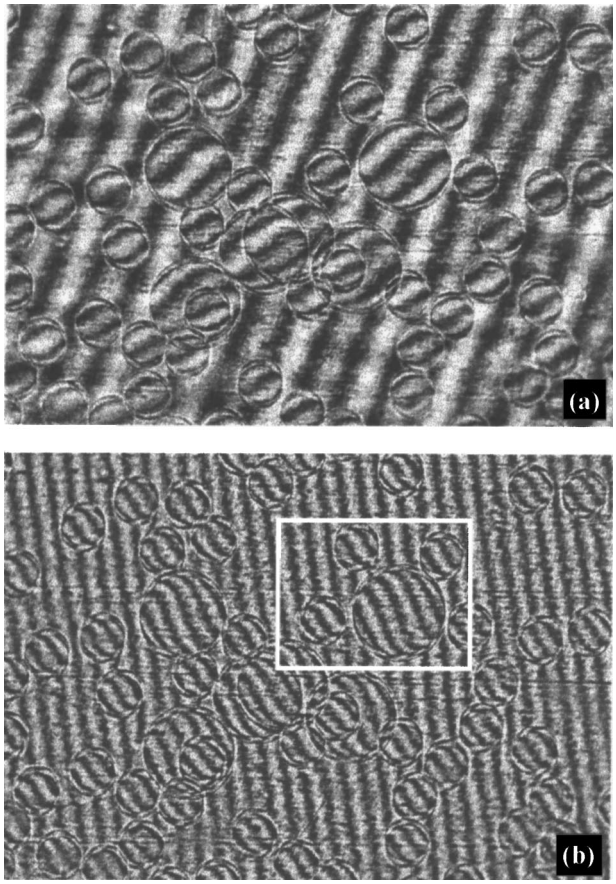

FIG. 5. Shearing interferograms of 100 and 200 μm diam polystyrene spheres taken at 12.4 keV photon energy for 0.3° (a) and for −0.7° angular misalignment (b).

$+I_{\min})=0.31$ independent of the photon energy. Although we did not take special precautions to stabilize the setup, no changes in the moiré patterns were observed even over several hours. The robustness of our shearing interferometer compared a to Mach–Zehnder-type setup lies in the fact that the grating constants involved and thus the stability tolerances are more than three orders of magnitude larger. The density of the moiré lines depended on the angular alignment of the gratings around the optical axis. Unfortunately, even for zero misalignment horizontal moiré lines with a pitch of 560 μm were recorded. This is caused by the fact that the incoming light is spherical rather than a plane wave. This causes detuning in the pitch of the interference lines p_i and the analyzer grating p_a by $p_i - p_a \approx d/r = 1.75\times10^{-3}$.

As a first application we recorded interferograms of 100 and 200 μm diameter polystyrene spheres as well defined phase objects to investigate this effect [see Figs. 5(a)–5(c)]. The interferograms show double contours of the spheres offset by $s=14$ μm along the vertical direction. Moreover, a change of the orientation of the moiré lines is observed inside the spheres, and it is directly linked to the difference in phase of the two interfering beams, i.e., the vertical phase gradient.

The interferograms obtained were compared with numerical simulations based on a wave propagation routine. Figure 6(a) shows the calculated image of six spheres distributed like in the region marked of Fig. 5(b) for the same photon energy and grating misalignment. The best match between the experimental and calculated data was obtained for $\delta=1.67\times10^{-6}$, where $n=1-\delta-i\beta$ is the complex refractive index. This is in good agreement with the value of $\delta=1.61\times10^{-6}$ tabulated for polystyrene with chemical composition of $[C_8H_8]_n$ and density of 1.11 g/cm^3.[12]

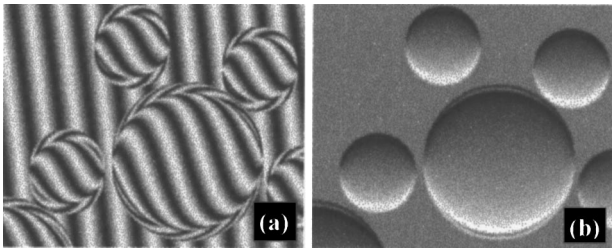

FIG. 6. Numerical simulations of the region marked in Fig. 5(b) for 12.4 keV photon energy and −0.7° angular misalignment (a) and for 24.8 keV photon energy, no angular misalignment, and grating pitch compensated for beam divergence (b).

The excellent agreement of the calculated and experimentally obtained interferograms indicates that quantitative analysis of an unknown phase object should be possible. In future work, we intend to use phase gratings with slightly different pitches to compensate for the divergence of the x-ray beam, which will greatly facilitate evaluation of the shearing micrographs. Figure 6(b) shows a calculated image of the same polystyrene spheres as it would appear for divergence matched phase gratings without any angular misalignment. The brightness at the horizontal edges of the spheres changes according to the sign and magnitude of the phase gradient. For small phase shifts, such a differential phase image can be turned into a phase image by simple integration along the shearing direction. We believe that this technique will prove to be useful in microradiography and microtomography, because it enhances the contrast of low absorbing specimens. For medical applications especially, this would help significantly in reducing the radiation dose applied.

The authors wish to thank B. Haas, A. Grubelnik, and R. Widmer for their support in fabricating the Si phase gratings. They also acknowledge T. Wilhein and P. Cloetens for fruitful discussions on interferometry.

[1] G. Schmahl, D. Rudolph, P. Guttmann, G. Schneider, J. Thieme, and B. Niemann, Rev. Sci. Instrum. **66**, 1282 (1995).
[2] A. Snigirev, I. Snigreva, V. Kohn, S. Kuznetsov, and I. Schelokov, Rev. Sci. Instrum. **66**, 5486 (1995).
[3] P. Cloetens, M. Pateyron-Salomé, J. Y. Buffiere, G. Peix, J. Baruchel, F. Peyrin, and M. Schlenker, J. Appl. Phys. **81**, 5878 (1997).
[4] K. A. Nugent, T. E. Gureyev, D. F. Cookson, D. Paganin, and Z. Barnea, Phys. Rev. Lett. **86**, 5827 (2001).
[5] P. Cloetens, W. Ludwig, J. P. Guigay, P. Pernot-Rejmankova, M. Salomé-Pateyron, M. Schlenker, J. Y. Buffière, E. Malre, and G. Peix, J. Phys. D **32**, 145 (1999).
[6] U. Bonse and M. Hart, Appl. Phys. Lett. **6**, 155 (1965).
[7] M. Ando and S. Hosoya, in *Proceedings of the 6th International Conference on X-Ray Optics and Microanalysis*, edited by G. Shinoda, K. Kohra, and T. Ichinokawa (University of Tokyo Press, Tokyo, 1972), pp. 63–68.
[8] A. Momose, T. Takeda, and Y. Itai, Rev. Sci. Instrum. **66**, 1434 (1995).
[9] F. Beckmann, K. Heise, B. Kölsch, U. Bonse, M. F. Rajewsky, M. Bartscher, and T. Biermann, Biophys. J. **76**, 98 (1999).
[10] C. David, E. Ziegler, and B. Nöhammer, J. Synchrotron Rad. **8**, 1054 (2001).
[11] C. David, B. Nöhammer, and E. Ziegler, Appl. Phys. Lett. **79**, 1088 (2001).
[12] B. L. Henke, E. M. Gullikson, and J. C. Davis, At. Data Nucl. Data Tables **54**, 181 (1993).